Effects of sintering temperature on composition, microstructure and electrochemical performance of spray pyrolysed LSC thin film cathodes

Author(s):
Pecho, Omar; Holzer, Lorenz; Yáng , Zhèn; Martynczuk, Julia; Hocker, Thomas; Flatt, Robert J.; Prestat, Michel

Publication date:
2014

Permanent link:
https://doi.org/10.3929/ethz-a-010286812

A1104

Effects of sintering temperature on composition, microstructure and electrochemical performance of spray pyrolysed LSC thin film cathodes

Omar Pecho[1,2] Lorenz Holzer[1], Zhèn Yáng[2], Julia Martynczuk[2], Thomas Hocker[1], Robert J. Flatt[3] and Michel Prestat[1,2]

(1) Institute of Computational Physics, Zurich University of Applied Sciences (ZHAW), Wildbachstrasse 21, 8401 Winterthur, Switzerland.

(2) Nonmetallic Inorganic Materials, ETH Zurich, 8093 Zurich, Switzerland.

(3) Institute for Building Materials, ETH Zurich, 8093 Zurich, Switzerland.

Tel.: +41-58- 934-7790

pech@zhaw.ch

Abstract

Thin nanoporous LSC ($La_{0.6}Sr_{0.4}CoO_{3-\delta}$) cathodes are deposited by spray pyrolysis onto gadolinium-doped ceria (GDC) electrolyte substrates, followed by sintering at 600°C, 800°C, and 1000°C. The investigation includes quantitative microstructure analysis, electrochemical characterization and application of Adler-Lane-Steele (ALS) model in order to extract intrinsic material properties and to explain the effects of variation in sintering temperature. A secondary gray phase (SGP) is detected, which consists of Sr and O and has a contrast in backscatter imaging intermediate between the pores and the LSC. SGP fills 66% of the mesopores in LSC sintered at 600 °C. With increasing sintering temperature the amount of SGP decreases until it disappears at 1000 °C. In this investigation we intend to understand the effect of SGP formation. For this purpose the influence of microstructural changes (i.e. active surface area) and variation of intrinsic material properties (exchange flux density) associated with SGP formation need to be quantified.

The area specific resistance (ASR) of symmetrical LSC/GDC/LSC cells is measured between 400 and 600°C by impedance spectroscopy. ASR values as low as 0.13 $\Omega \bullet cm^2$ are obtained for samples sintered at 600°C, and 80 times higher for samples sintered at 1000 °C. These results indicate that the SGP is not blocking gas diffusion of O_2 in the pores and therefore surface oxygen reduction reaction may take place over the entire LSC surface. Hence at low sintering temperatures a high specific surface area is obtained and the results indicate that formation of SGP does not bring a negative effect neither on the oxygen transport in 1-µm thin electrodes, nor on the oxygen reduction kinetics of LSC. An inverse correlation between the measured ASR values and the LSC-surface is obtained. The exchange neutral flux density, r_0, is calculated using the ALS model, which results in r_0-values in the range between 10^{-8} (600°C) and 10^{-9} mol/cm^2/s (1000°C). Considering the formation of a secondary SrO-phase in a mass-balance for the entire sample also leads to the conclusion that there must be an increase of A-site deficiency and oxygen vacancies in LSC. In summary, it can be concluded that the variation of the ASR between LSC sintered at 600°C and 1000 °C is more strongly related to the difference in intrinsic material property, (r_0 varies by a factor of 40) than the difference in surface area, (a varies by a factor of 2). For a controlled optimization of cathode performance it is necessary to consider all these different aspects (non-stoichiometric compositions, microstructure, secondary phase formation, intrinsic properties, sintering temperature).

Introduction

Over the last several years, the development of solid oxide fuel cells (SOFC) progresses towards lower operating temperature, which encompasses both conventional and miniaturized SOFC applications [1-8]. Lowering the operating temperature has the benefits of slower rate of SOFC components degradation and reduced start-up time. Consequently, electrodes must be optimized to meet these demands. Microstructure must be designed to increase the number electrochemically active sites. Materials that exhibit high activity towards oxygen reduction are also desired especially at relatively low operating temperatures.
The electrochemical performance of cathodes is affected by two coupled phenomena: transport of mobile species (gas, ions and electrons) and oxygen reduction reaction at the surface. The overall kinetics of oxygen reduction is generally described as being limited by surface exchange at the electrode/air interface. Electrode activity can therefore be enhanced by using electrodes with mixed ionic-electronic conducting (MIEC) properties such as LSC [1,2,9-11], which can extend the reaction from the triple phase boundary at the electrolyte-electrode interface into the porous cathode layer. Moreover, utilization of thin film cathodes has attracted attention due to increased thermo-mechanical stability and reduced grain size due to the nanostructure.
In this work, thin LSC electrodes are deposited by wet spray pyrolysis. Microstructure characterization is done by scanning electron microscopy (SEM) and FIB-nanotomography. Local chemical compositions are analysed with TEM-EDX. The electrochemical performance is evaluated in terms of area specific resistance (ASR, symmetrical cells) obtained from impedance measurements. Moreover, the ASR and the specific surface area from image analysis are used as input in the ALS model to evaluate the neutral flux density, r_0.

1. Experimental

The precursor solution consisted of $La(NO_3)_3 \cdot 6H_2O$, $SrCl_2 \cdot 6H_2O$, $Co(NO_3)_2 \cdot 6H_2O$ (metal concentration 0.4 mol L^{-1}), which was dissolved in a mixture of 32 vol% ethanol, 63 vol% diethylene glycol monobutyl ether (DGME) and 5 vol% polyethyleneglycol (PEG600). The solutions were sprayed onto gadolinia-doped ceria (GDC, $Gd_{0.1}Ce_{0.9}O_{1.95}$, Kerafol®, 0.20 mm thick) tapes heated at 340°C with the set-up schematically described in Figure 1. The resulting LSC films were sintered at three different temperatures: 600 °C, 800 °C and 1000 °C for 4 hours in air. Focused ion beam – scanning electron microscope (FIB-SEM, Helios Nanolab 600i) was used for quantitative and qualitative characterization of the microstructures. Quantification of the phase sizes was done by continuous phase distribution (c-PSD, [12]) using in-house plugins for Fiji software and applying them to 2D-images from FIB-SEM. Specific surface and interface area was determined by measureing the corresponding phase perimeters from segmented 2D-images. Spot analysis and compositional mapping were done with TEM-EDX.

Symmetrical cells (LSC/GDC/LSC) were used to evaluate the ASR of the films measured by impedance spectroscopy. Measurements were done between 400-600 °C in steps of 50 °C in air. For the electrochemical measurements, a Solartron impedance analyser (SI1260) and a Solartron potentiostat (SI1287) were utilized.

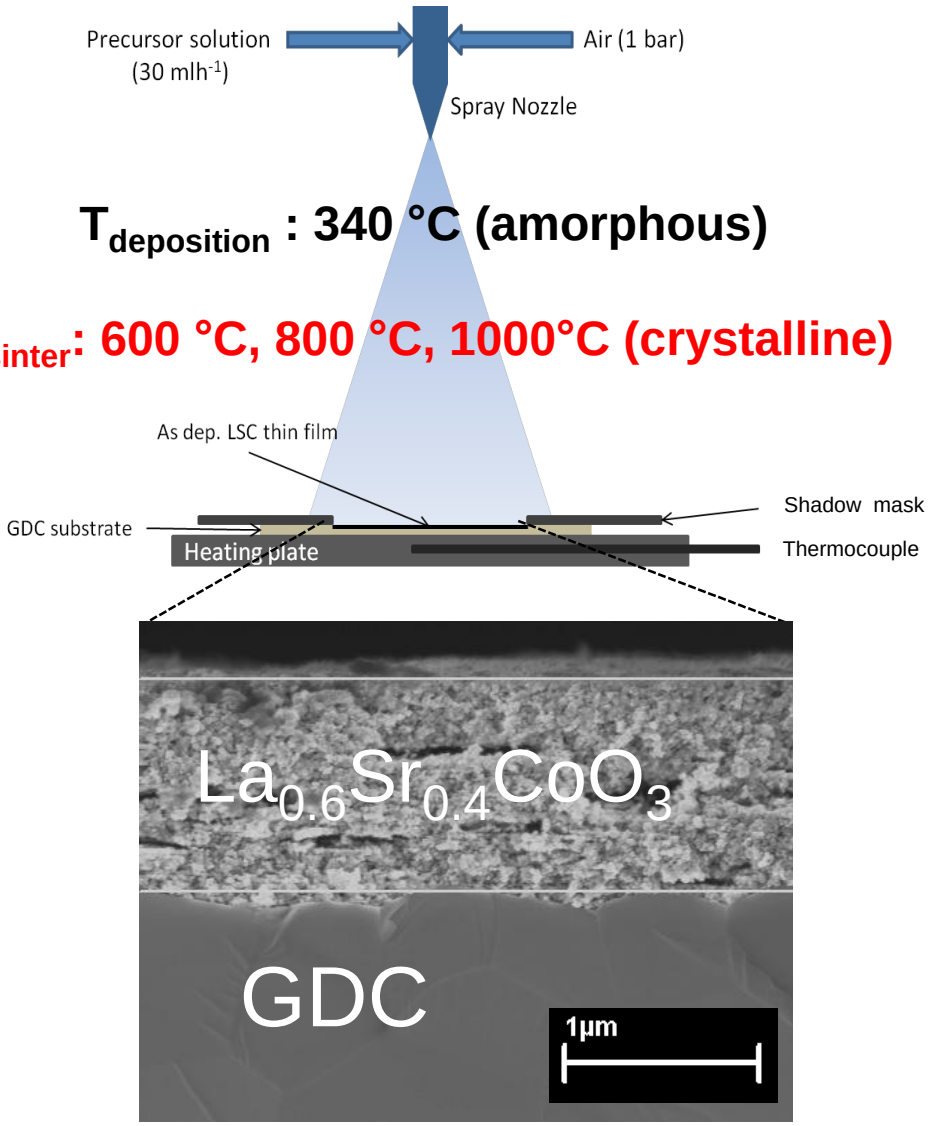

Figure 1. Deposition of thin LSC films on GDC substrates heated at 340 °C.

2. Results

The as-deposited amorphous films crystallized after sintering at the different temperatures and no delamination of cathode film was observed after sintering. At lower sintering temperature, the phases are smaller with elongated pores randomly distributed over the entire film thickness. As the sintering temperature increases, the phases become more isometric with significant coarsening especially between 800°C and 1000°C. However, single-phased LSC was not obtained. A secondary phase (SP), with contrast in backscatter imaging intermediate between the pores and LSC is observed (Figure 2). Quantitative microstructure analysis reveals that the amount of secondary phase is temperature-dependent. Significant volume fraction of the secondary phase was determined for the samples sintered at 600°C. The secondary phase is filling the pores and covering the LSC surface. This fraction decreases at 800 °C and disappears at 1000°C.

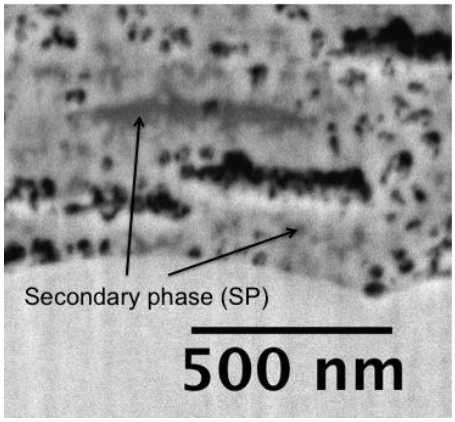

Figure 2. LSC obtained after sintering at 600°C. The secondary phase fills the pores and covers the surface of LSC.

Lowering the sintering temperature resulted to smaller phase sizes. Consequently, due to the smaller LSC phase size, the LSC surface area at 600°C is greater than at 1000°C. The ASR of LSC/GDC/LSC symmetrical cells were measured in air. The ASR values increased by a factor of 78 with higher ASR for samples sintered at 1000°C (Table 1). The relatively good ASR of the LSC cathode sintered at 600°C indicates that the approach of lowering the sintering temperature (phase size) is appropriate. However, the good electrochemical performance cannot be solely explained by the improvement in the microstructure (since the secondary phase is filling the pores). For a better understanding of the microstructure-property relationship in these samples the intrinsic properties of the secondary phase must be investigated. TEM-EDX analyses indicate that the secondary phase is composed of Sr and O. Under consideration of a mass balance for the entire sample, it must be assumed that LSC has a modified (non-)stoichiometry with associated Sr-deficiency on the A-site.

In order to evaluate semi-quantitatively the extent of Sr-deficiency in LSC we perform some mass balance calculations. For these calculations, we assume that the secondary phase is made of SrO, and that the specific volume of LSC does not change although a fraction of the Sr is not fully incorporated into the LSC lattice (only the stoichiometry changes). Using the molecular mass, density and amount of Sr not incorporated (given by x in $La_{0.6}Sr_{0.4-x}CoO_{3-\delta}$), the volume of the crystalline SrO-phase corresponding to a certain A-site deficiency can be calculated. Furthermore, we can then compare this calculated volume fraction for a crystalline SrO-phase with the measured volume fraction obtained by image analysis for the secondary phase. The results from mass balance calculation show that even at the maximum amount of Sr-deficiency (x=0.4, i.e. all Sr in the secondary phase), there would not be enough volume of a crystalline SrO-phase to occupy the whole volume of the secondary phase (from image analysis). This indicates that the bulk density of the observed secondary phase is much lower than the density of the crystalline SrO-phase.

For the series of samples sintered at different temperatures, it was found that the total surface area of LSC inversely correlates with the ASR. This indicates that the total surface area of LSC is electrochemically active, and hence the secondary phase, which fills the pores in the better performing samples (600°C), must be permeable to gas. The mass balance calculations as well as the backscatter contrast indicate that the density of the secondary phase is very low, most probably due to finely dispersed nanoporosity. This may explain why the secondary phase has a high permeability for oxygen-diffusion. The

distribution of secondary phase in the sample sintered at 600°C is shown in Fig. 3, based on 3D-images from FIB-tomography. The simulation shown in Fig. 3 (D) was performed under the assumption that the secondary phase is a dense material, which leads to an apparent disconnection of the pores from the cathode surface. Oxygen can only diffuse into the sample if the secondary phase is permeable.

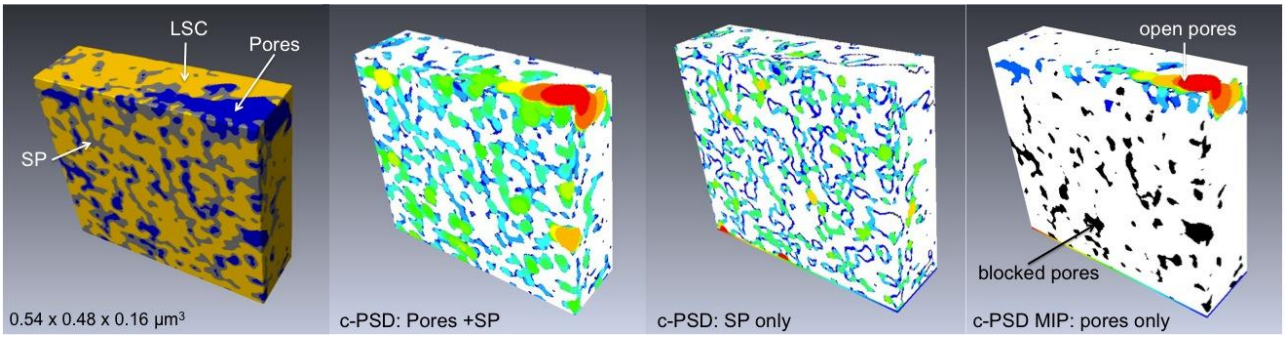

Figure 3. (A) Segmented 3D structure of LSC sintered at 600°C from FIB-tomography. (B) Color-coded distance maps for combined pores+secondary phase segmentation. (C) Distance maps for secondary phase. Note: surface coverage of pore-walls in blue. (D) simulation of mercury intrusion and correspoding distance map. Note: black represents pores disconnected from the cathode surface due to blocking by secondary phase.

As mentioned, the formation of the secondary phase affects not just the microstructure but also the non-stochiometry and associated intrinsic material property. As summarized in Table 1, the difference (factor of 78) between the ASRs of the LSC cathodes sintered at 600 °C and 1000 °C cannot be solely explained by microstructure (because the surface area varies only by a factor of 2). For our thin films the simplified version of the Adler-Lane-Steele model is applicable, since the whole layer thickness is electrochemically active (i.e. the calculated utilization region is greater than 1 µm). The neutral flux density, $r_{0,}$ can then be resolved by substituting the values of the surface area obtained from image analysis and the ASR obtained from EIS measurements into equation 1.

$$ASR = \frac{RT}{4F^2}\frac{1}{aLr_0\left(\alpha_f + \alpha_b\right)} \qquad \text{(equation 1)}$$

The results summarized in Table 1 show, that the neutral flux density (r_0), which is a kinetic material property of the materials, changes by factor of 39 from LSC cathodes sintered at 600 °C to 1000 °C. This indicates that the understoichiometry and Sr-deficiency is beneficial to the electrochemical performance of LSC.

Table 1. Summary of quantitative microtructural and electrochemical characterization of 1-µm thin film LSC cathodes

T_{sinter}	600 °C	factor	1000 °C
LSC total surface area (μm^{-1})	28.9	2	14.3
ASR ($\Omega \cdot cm^2$)	0.13	78	10.1
SGP volume fraction (%)	20.7		0
Non-stoichiometry	Yes		No
Intrinsic property, r_0 ($mol/cm^2/s$)	$5.20 \cdot 10^{-8}$	39	$1.35 \cdot 10^{-9}$

3. Conclusion

This work has successfully demonstrated that lowering the post-deposition sintering temperature results to lower phase sizes in the cathode nanostructures. Consequently, the available surface also increases thereby enhancing the electrochemical kinetics. However, as a consequence of lowering the sintering temperature some of the Sr is not incorporated into the LSC lattice. As a result, a secondary phase composed of Sr and O is observed in backscatter imaging. The inverse correlation between the total LSC specific surface and ASR measurements indicates that the secondary phase is not blocking gas diffusion. Furthermore, mass balance calculations indicate that the secondary phase is not a dense SrO-phase, but contains a high fraction of nanoporosity, making it permeable for oxygen diffusion. The amount of secondary phase is also linked with the A-site deficiency in LSC, which brings changes in the intrinsic material property of the LSC. In particular, the neutral flux density resolved from ALS model shows that r_0 increases with decreasing sintering temperature and associated A-site deficiency. These results show that lowering the sintering temperature is beneficial for both the microstructure and the intrinsic material property, whereby the latter is dominating the enhanced electrochemical properties in LSC sintered at 600°C.

Acknowledgement

The authors thank P. Gasser, G. Peschke and the Electron Microscopy Center of ETH Zurich (EMEZ) for the help with the FIB. The financial support from the Swiss National Science Foundation (contracts CRSI22-126830 and 200021-135270) is gratefully acknowledged.

References

[1] J. Hayd *et al.*,*J. Power Sourc.*, 196 (2011) 7263.
[2] H.S. Noh *et al.*, *J. Power Sourc.,* 247 (2014) 105.
[3] M. Prestat *et al.*, *Proc. of the 10th Eur. Fuel Cell Forum*, Eds. F. Lefebvre-Joud *et al.*, Lucerne, Switzerland (2012), p. A07-30.
[4] A. Evans *et al.*, *J. Power Sourc*., 194 (2009) 119.
[5] B.K. Lai *et al.*, *J. Power Sourc.*, 196 (2011) 1826.
[6] P.C. Su, F.B. Prinz, *Electrochem. Commun.,* 16 (2012) 77.
[7] C. Chao *et al.*, *ACS Nano*, 5 (2011) 5692.
[8] Y. Yan *et al.*, *J. Power Sourc.,* 206 (2012) 84.
[9] A. Evans *et al.*, *Fuel Cells*, 13 (2013) 441.
[10] I. Garbayo *et al.*, *J. Power Sourc.*, 248 (2014) 1042.
[10] G. Gaiselmann *et al., Comp. Mater. Sci.,* 67 (2013) 48.
[12] B. Münch,L. Holzer, *J. Am. Ceram. Soc.,* 91 (2008) 4059 - 4067.